Journal of materials and Environmental Sciences
ISSN : 2028-2508

JMES, 2017 Volume 8, Issue 1, Page 345-355

http://www.jmaterenvironsci.com/

Adsorption of Rhodamine B Dye onto Expanded Perlite from Aqueous Solution: Kinetics, Equilibrium and Thermodynamics

B. Damiyine*, A. Guenbour, R. Boussen*

Laboratory of Materials Nanotechnology and Environment, Department of Chemistry, Faculty of Science, University Mohammed V, BP1014, Rabat, Morocco.

Received 21 Jul 2016,
Revised 13 Nov 2016,
Accepted 15 Nov 2016

Keywords :
- Kinetics studies,
- Adsorption isotherm,
- Expanded Perlite,
- Rhodamine B,
- Sorption

1. Introduction

ratiba20@gmail.com;
Phone: +2126 60614610,
Brahimgp@gmail.com;
Phone: +212 6 61950835

Abstract

Batch sorption kinetics of Rhodamine B (RB) by Expanded Perlite (EP) has been studied in terms of pseudo- first-order, pseudo-second-order and intra-particle diffusion models. The results showed that sorption process was best described by the pseudo-second-order model. The correlation coefficients R^2 obtained from pseudo-second-order model were higher than 0.97 under all the experiment conditions. The effect of initial dye concentration, contact time, solution temperature and pH solution on kinetic parameters are discussed. Thermodynamic studies and adsorption isotherms Langmuir, Freundlich and Temkin were used to describe this phenomenon of adsorption. The adsorption process was followed by UV-spectrophotometric technique in a specially designed adsorption cell. The results show that Expanded Perlite is a good adsorbent for the removal of Rhodamine B from aqueous solutions. The quantity eliminated was depended on the initial concentration, contact time, solution temperature and pH of solution.

1. Introduction

Pollution caused by industrial wastewater has become a common problem in all countries. Especially, organic pollution dye industrial effluent cause risk to human health and ecological balance.

For this purpose, many methods such as activated carbon sorption, chemical coagulation, ion exchange, electrolysis, biological treatment, have been developed [1] [2] to eliminate undesirable pollution.

In this work, the EP powder was crushed, sieved at 90 microns have been selected as a sorbent for the study of kinetics sorption of RB dye from aqueous solution.

Perlite is a volcanic rock glass ranging in color from gray to black, when heated to high temperatures (800°C - 1100°C), it expands up to 35 times its internal volume and it is called "Expanded Perlite" [3]. This product has a low density, high surface area, and low thermal conductivity [4]. In addition, since most of the perlite samples have a high silica content (over 70%), they have adsorbent properties [5].

The adsorbent nature of perlite is due to the silanol groups, which are formed by silicon atoms on the surface of the perlite. The types of silanol groups are represented as follows [6]:

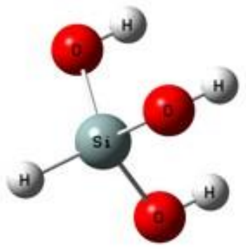

Hydroxyl or silanol groups

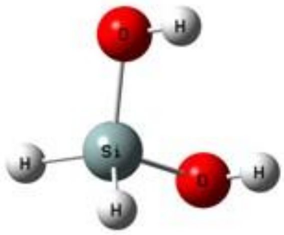

Silanediol groups

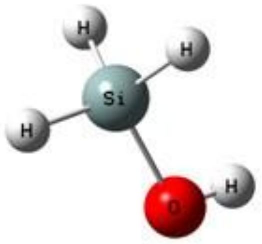

Silanetriol groups

The hydrous oxide surface groups in alumina are given as follows [5]:

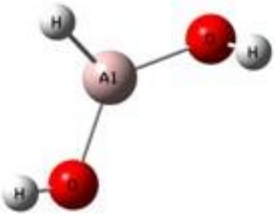

Or

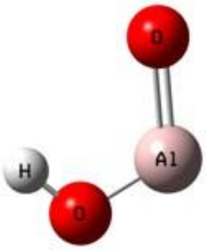

The silicon atoms at the surface tend to maintain their tetrahedral coordination with oxygen. They complete their coordination at room temperature by attachment to monovalent hydroxyl groups, forming silanol groups. The surface of perlite becomes more negatively or positively charged according to the pH of the solution medium. This situation affects sorption capacity.

Also, EP is used as an excellent filter aid and as filler in various processes and materials [7] since they are chemically inert.

The present study is aimed to study a convenient and economic method for RB removal from water by adsorption on a low cost and an abundantly available adsorbent, to gain an understanding of the adsorption kinetics, to describe the rate and mechanism of adsorption, to determine the factors controlling the rate of adsorption and to calculate the activation energy of system. The effects of solution pH, initial concentration, contact time and solution temperature on RB adsorption rate have been evaluated.

1. Materials and methods

2.1. *Material characterization*

The EP sample was obtained from Dicalite Europe nv, Scheepzatestraat 100, 9000 Gent, Belgium, company ISO 9001: 2008 certified. The EP sample was sieved by 90-mesh sieve and dried at 110 °C for 1 h. The chemical composition of the perlite which was determined by FT-IR, EDX, and XRF* (*was determined according to literature) [8] are given in figure 1, 2 and Table 1. The FT-IR spectra were of recorded at 400−4000 cm^{-1} wave number range using a FT-IR spectrometer (BRUKER, model: Tensor 27) and The Energy Dispersive X-ray (EDX) analysis was performed using HORIBA XGT-1000.

The IR bands of wavelength 1000 cm^{-1}, and 470 cm^{-1} are bands characteristics of the silicon that is major element of Perlite.

The Perlite images before and after adsorption were carried out by digital microscope Leica DVM5000 HD, figure 3.

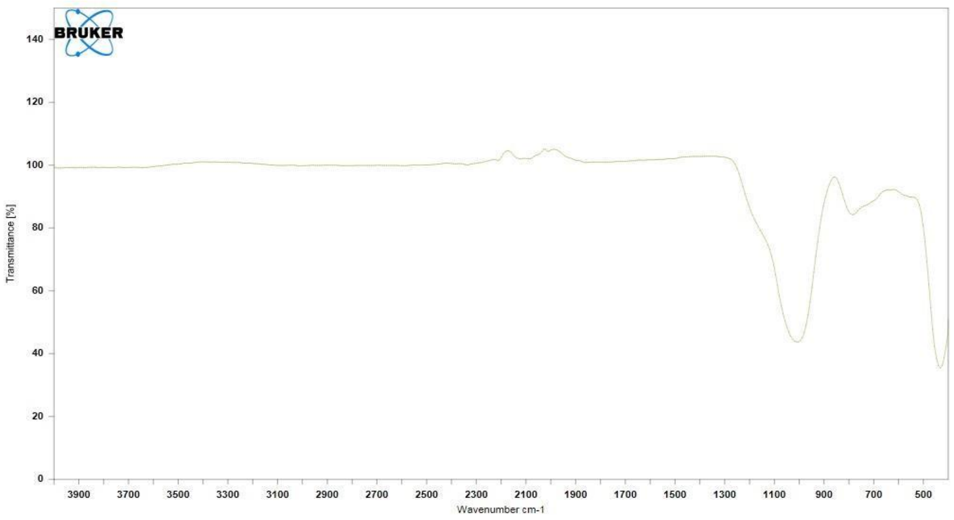

Figure 1: FT-IR spectrum of Expanded Perlite sample

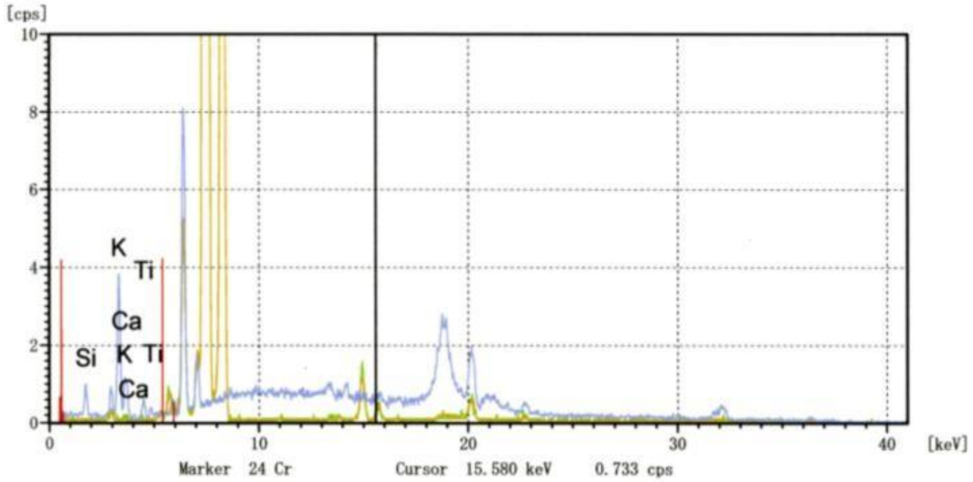

Figure 2: EDX spectrum of Expanded Perlite sample

Table 1: Chemical composition of Expanded Perlite

Major Elements	Composition (Wt %)
SiO_2	74.75
Al_2O_3	12.48
Fe_2O_3	0.88
Na_2O	4.48
K_2O	5.42
CaO	0.7
MgO	0.1
TiO_2	0.06

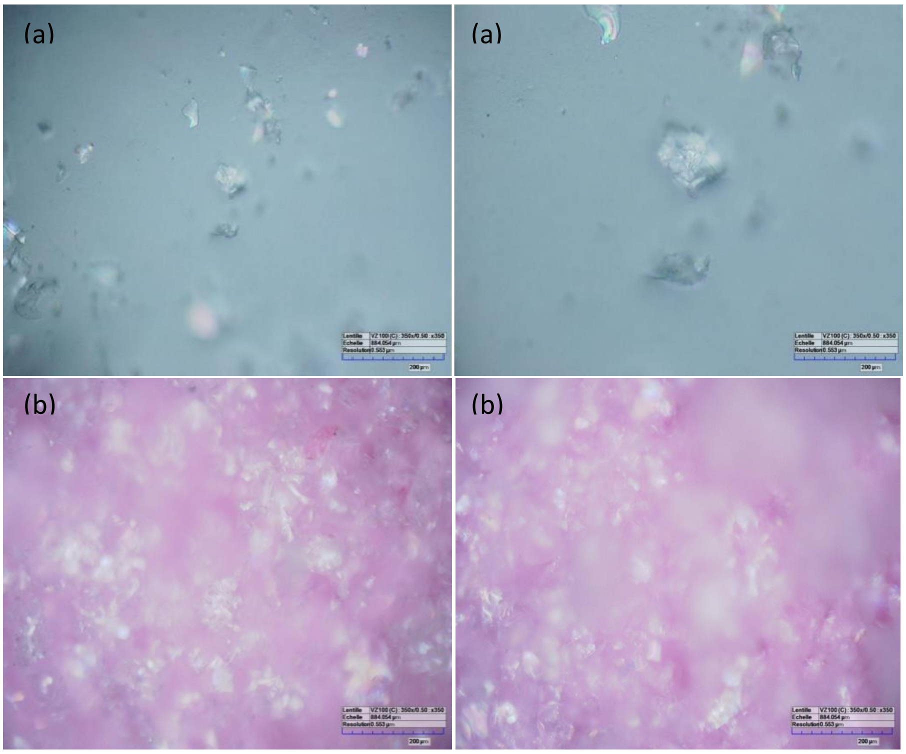

Figure 3: Digital Microscopy images of EP (a) before adsorption and (b) after adsorption

2.2. *Rhodamine B*

Rhodamine B is a cationic dye, purchased from Merck Millipore Corporation, Germany. The structure of dye is shown in Figure 4. The absorbance maximum is 554 nm.

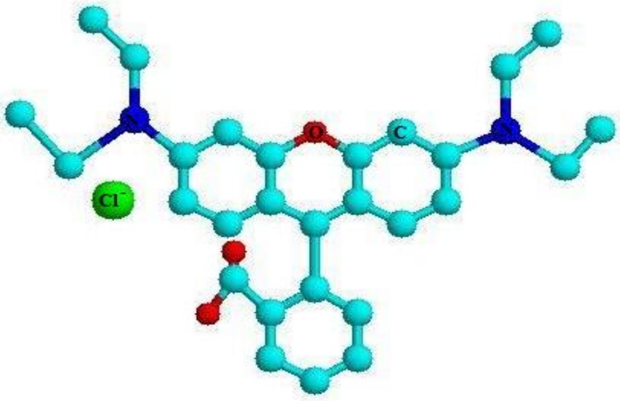

Figure 4: Structural formula of Rhodamine B

The batch mode adsorption studies were carried out to study the effect of parameters like initial concentration, contact time, solution temperature and pH of solution for the removal of RB dye. Batch adsorption experiments were carried by adding 0.5 g of EP into 250 mL in Erlenmeyer flasks containing 50 mL of different initial concentrations of RB solution. The flasks were agitated at 500 rpm. The adsorbent was separated and centrifuged at 3000 rpm for 15 min, the concentration of RB in supernatant was determined at a wavelength of maximum adsorption (λmax) at 554 nm by visible spectrophotometer (Jasco V-670 spectrophotometer). The amount of adsorbed dye at equilibrium qe (mg/g) and the removal percentage were calculated by the following equations:

$$qe = (C_0\text{-}Ce).V/ W \qquad (1)$$

$$\%\ removal = ((C_0\text{-}C_e)/C_0) \times 100 \qquad (2)$$

Where C_0 and C_e are the initial and equilibrium concentrations of dye, respectively (mg/L). V is the volume of dye solution (L) and W is the weight of adsorbent used (g).

2. Results and discussion

3.1. *Effect of contact time*

Figure 5 shows the adsorption percentage of RB as a function of contact time. As seen in this figure, adsorption of this dye increased by contact time and reached to a maximum value (82%). More increase in contact time had more sensible changes in adsorption percentage. Hence, adsorption of RB reached their maximum at 180, 210 and 240 min, respectively. These values have been selected as optimum contact time.

3.2. *Effect of pH*

The pH of the dye solution is one of the most important parameter as the protonation of functional groups on adsorbent surface and the chemistry of dye molecules are strongly affected by pH of the solution. The effect of initial pH on the adsorption of RB by EP was studied by varying the pH of dye solution from 2 to 12 for initial concentration of 10 mg/L (Figure 6). It is evident from the figure that the sorption capacity of EP decreased from 47 to 86.5 % with increase in solution pH 2 to 12.

Therefore, the pH for 7 to 12 was selected as an optimum pH for this experiment.

3.3. *Effect of temperature*

The results of the studies on the influence of temperature on RB adsorption is presented in Figure 7.

The batch mode adsorption studies were carried out to study the effect of temperature for the removal of RB dye. Batch adsorption experiments were carried by adding 0.5 g of EP into 250 mL in Erlenmeyer flasks containing 50 mL of solution at different temperature 20°C, 30°C, 40°C, 50°C and 60 °C.

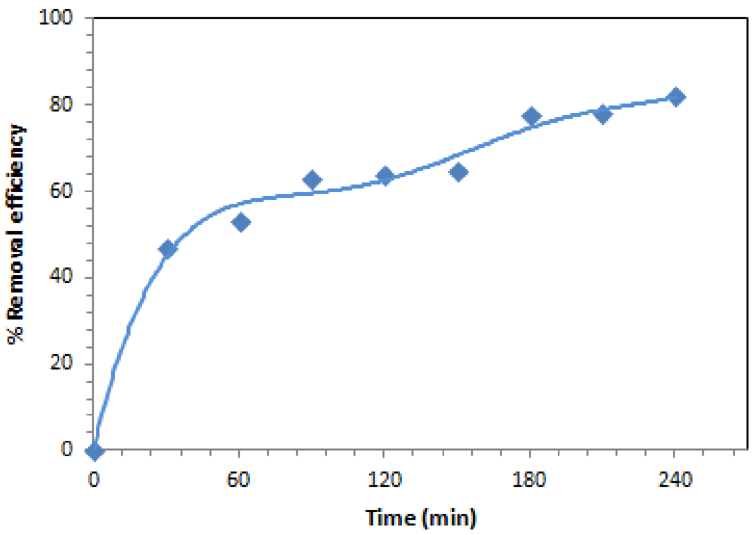

Figure 5: Effect of contact time on adsorption of RB onto EP (adsorbent dose = 0.5 g/50 mL, C = 10 mg/L, T=20°C)

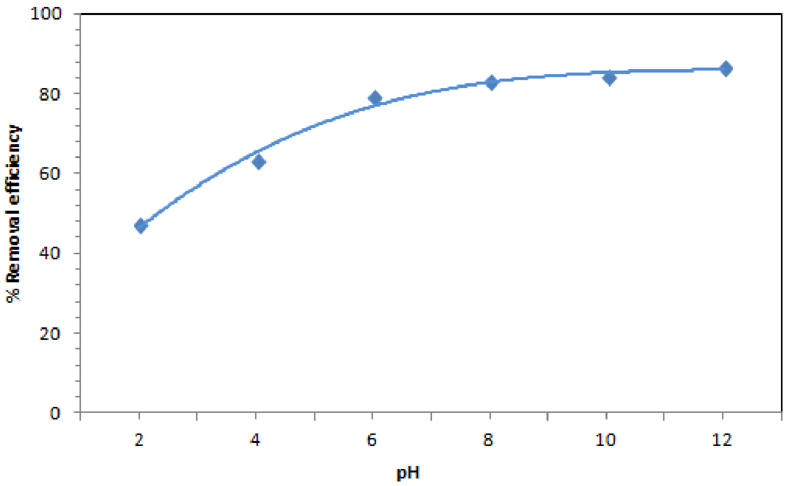

Figure 6: Effect of pH on the removal of RB (adsorbent dose = 0.5 g/50 mL, C = 10 mg/L, t = 60 min, T=20°C)

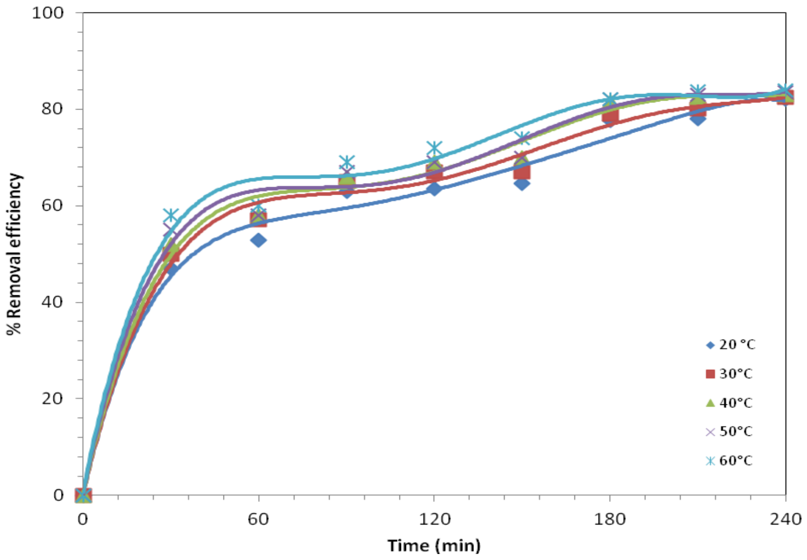

Figure 7: Effect of temperature on the adsorption kinetics of RB onto EP (adsorbent dose = 0.5 g/50 mL, C_0=10mg/L, pH=7)

A study of the temperature dependence of adsorption reactions gives valuable information about the enthalpy and the entropy change during adsorption.

The adsorption of RB onto EP indicating that the phenomenon of removal of RB onto EP is endothermic in nature when temperature was increased from 20 to 60 °C (Figure 7) at pH = 7 and C_0 = 10mg/L. The increase in the equilibrium sorption of dye with temperature indicates that dye removal by adsorption on EP favor’s a high temperature [9]. This may be a result of increase in the mobility of the large dye ion with temperature.

An increasing number of molecules may also acquire sufficient energy to undergo an interaction with active sites at the surface. Furthermore, increasing temperature may produce a swelling effect within the internal structure of the EP enabling large dyes to penetrate further [10].

3.4. *Effect of the initial concentration of dye*

The effect of initial concentration on RB removal by studied adsorbents is shown in Figure 8. It can be seen that the adsorption capacity of RB dye by studied adsorbents increases with an increase in the initial RB dye concentration, and then approaches a fixed value. The increase of adsorption capacity with raising the initial RB dye concentration is due to an increase of the numbers of RB dye molecule available to binding sites of adsorbents. At higher RB dye concentration, the active sites become saturated and adsorption capacity approaches a constant value.

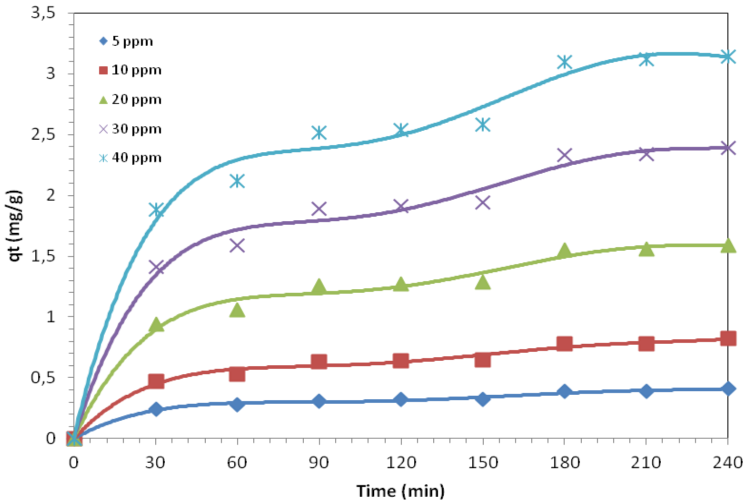

Figure 8: Effect of concentration of RB on adsorption onto EP (adsorbent dose = 0.5 g/50 mL, T=20°C)

3.5. *Adsorption isotherm*

The adsorption isotherm represents the quantity adsorbed according to the concentration of the aqueous solution to equilibrium at a given temperature. Firstly the isotherms models of adsorption are generally used to describe the interactions between the adsorbate and the adsorbent when the process of adsorption reaches equilibrium. Secondly, they make it possible to extract the important parameters for the systems design from adsorption. The data of adsorption were analyzed by the three models of isotherms, Freundlich, Langmuir and Temkin.

3.5.1. *Langmuir adsorption isotherm*

The Langmuir isotherm assumes monolayer adsorption on a uniform surface with a finite number of adsorption sites. Once a site is filled, no further adsorption can take place at that site. As such the surface will eventually reach a saturation point where the maximum adsorption of the surface will be achieved [11]. The linear form of the Langmuir isotherm model is described [12] as:

$$\frac{Ce}{Qe} = \frac{1}{K_L Qm} + \frac{1}{Qm} Ce \qquad (3)$$

Where Ce is the equilibrium concentration in the solution (mg/l), Qe is the equilibrium uptake on the adsorbent (mg/g), Qm is the maximum adsorption capacity (mg/g), and K_L is the Langmuir constant that is related to the affinity of binding sites and is related to the energy of sorption (l/g). These constants can be determined from the linear plot Ce/Qe versus Ce, which has a slope of 1/Qm and the intercept of $1/K_L Qm$ (Figure 9).

From the regression correlation coefficient (R^2) values that are regarded as a measure of the goodness of fit of experimental data on the isotherm's model (Table 2), it illustrates that the Langmuir equation represents RB adsorption process on EP at the different solution temperatures very well, the R^2 values that ranged between 0.97 and 0.989, indicating a good mathematical fit. On the other side it may be predicted from Table 2 that the removal of RB onto EP is an endothermic process. Where monolayer sorption capacity of RB (Qm) increased as solution temperature was increased.

The essential characteristic of the Langmuir isotherm can be evidenced by the dimensionless constant called equilibrium parameter, R_L.

$$RL = \frac{1}{1+KLC0} \qquad (4)$$

Where K_L is the Langmuir constant C_0 is the initial RB concentration, R_L values indicate the type of isotherm to be irreversible ($R_L = 0$), favorable ($0 < R_L < 1$), linear ($R_L = 1$) or unfavorable ($R_L > 1$) [13].

In this study, all R_L values obtained were equal one as shown in Table 2. These values support the previous observation where the Langmuir isotherm was linear for RB adsorption for all studied temperatures.

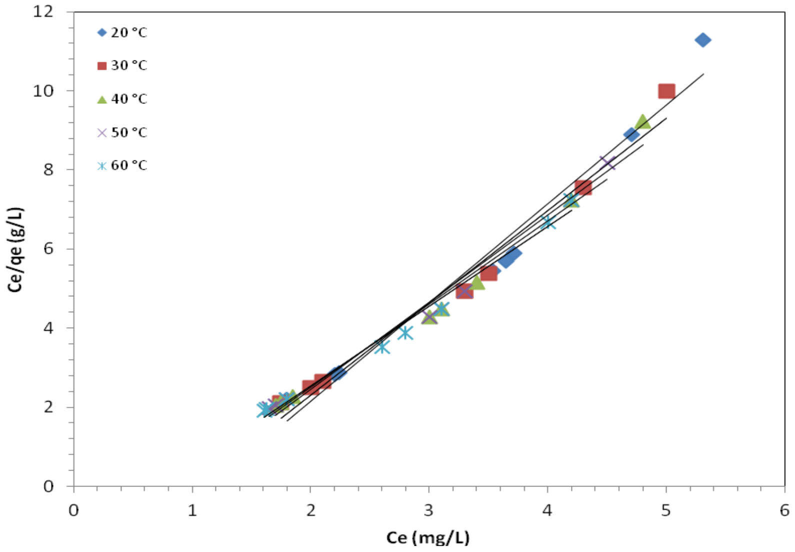

Figure 9: Langmuir isotherm for RB adsorption onto EP

3.5.2. *Freundlich adsorption isotherm*

The obtained experimental RB uptake values have also been analyzed using Freundlich equation. The Freundlich isotherm model is valid for multilayer adsorption on a heterogeneous adsorbent surface with a no uniform distribution of heat of adsorption. Freundlich isotherm can be expressed by: [14].

$$\log Qe = \log K_F + \frac{1}{n} \log Ce \qquad (5)$$

Where n and K_F are Freundlich constants related to adsorption intensity and adsorption capacity, respectively. The Freundlich constants K_F and n are obtained from the plot of log Qe versus log Ce that should give a straight line with a slope of 1/n and intercept of log K_F. From Figure 10, a linear relation was observed among the plotted parameters at different temperatures.

3.5.3. *Temkin adsorption isotherm*

The Temkin isotherm model assumes the adsorption energy decreases linearly with the surface coverage due to adsorbent–adsorbate interactions. The linear form of Temkin isotherm model [15] is defined by:

$$q_e = B \ln Kt + B \ln C_e \qquad (6)$$

Where B_t is the Temkin constant related to heat of adsorption (kJ/mol) and K_t is the Temkin isotherm constant (L/g). These constants were obtained from plotting Qe versus $\ln(C_e)$ Figure 11. Values of B_t and K_t are listed in Table 2.

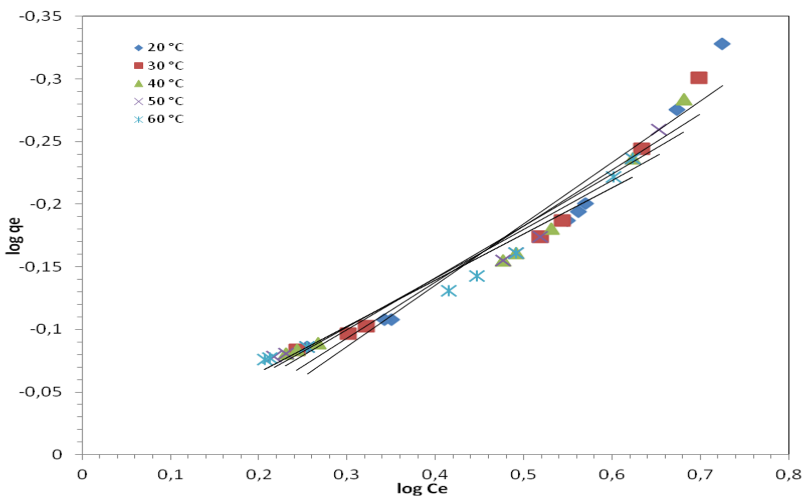

Figure 10: Freundlich isotherm for RB adsorption onto EP

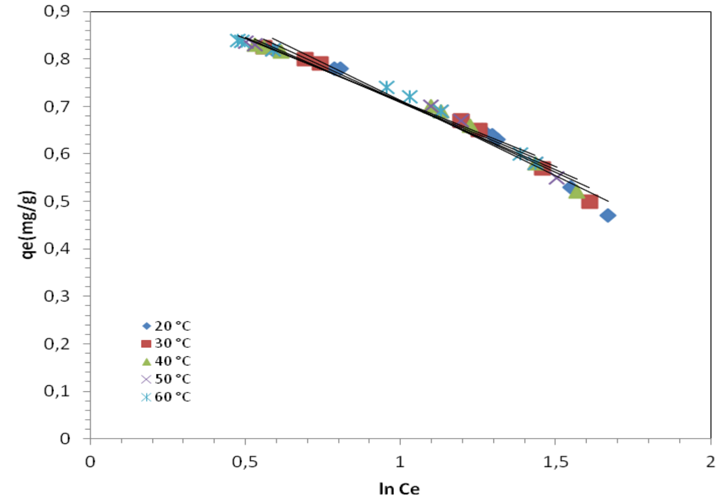

Figure 11: Temkin isotherm for RB adsorption onto EP

Table 2: Adsorption isotherm constants for RB adsorption onto EP

T(C°)	Langmuir isotherm constants				Freundlich isotherm constants			Temkin isotherm constants		
	q_m (mg/g)	K_L ($L{\cdot}g^{-1}$)	R^2	R_L	K_F (mg/g (L/mg)$^{1/n}$)	n	R^2	K_t ($L{\cdot}g^{-1}$)	B_t (KJ/mol)	R^2
20	0.3998	-0.8768	0.9711	1.00	1.0628	-2.0395	0.9439	0.0388	-0.3172	0.9751
30	0.4294	-0.9939	0.9762	1.01	1.0424	-2.2300	0.9520	0.0343	-0.2996	0.979
40	0.4526	-1.1230	0.9799	1.01	1.0249	-2.4166	0.9551	0.0300	-0.2834	0.9795
50	0.4754	-1.2418	0.9851	1.01	1.0149	-2.5674	0.9631	0.0273	-0.2725	0.9825
60	0.4954	-1.3440	0.9890	1.01	1.0084	-2.7100	0.9657	0.0245	-0.2629	0.9822

3.6. *Adsorption kinetics*

Three simplified kinetic models were adopted to examine the mechanism of the adsorption process. First, the kinetics of adsorption was analyzed by the pseudo-first-order equation given by Lagergren [16] :

$$\log(qe\text{-}qt)=\log(qe)\text{-}\left(\frac{K_1}{2.303}\right)t \qquad (7)$$

Where qe and qt are the amounts of RB adsorbed (mg/g) at equilibrium and at time t (h), respectively, and k_1

($g.mg^{-1}.h^{-1}$) is the rate constant adsorption. Values of k_1 at 20°C were calculated from the plots of $\ln(qe - qt)$ versus t (figure 12) for different initial concentrations of RB. The R^2 values obtained were relatively small and the experimental qe values did not agree with the calculated values obtained from the linear plots (Table 3).

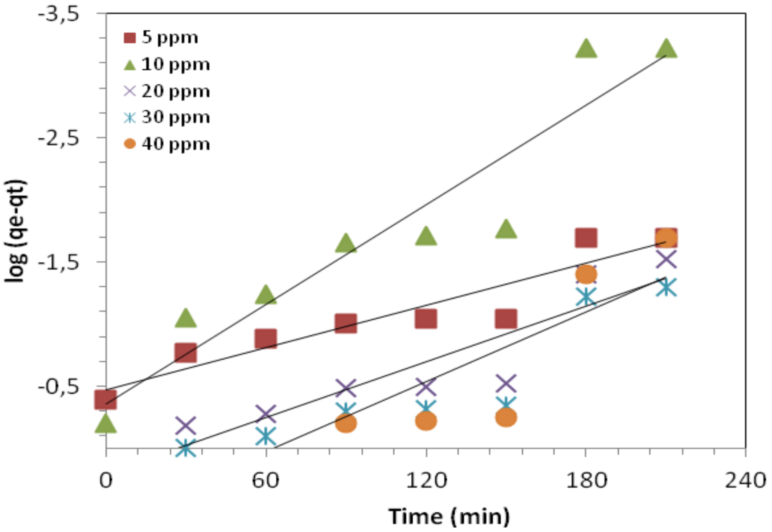

Figure 12: Pseudo-first order kinetic model for RB adsorption onto EP at different initial concentrations

On the other hand, the pseudo-second-order equation based on equilibrium adsorption [17] is expressed as:

$$\frac{1}{qt} = \frac{1}{K_2 q_e^2} + \left(\frac{1}{qe}\right)t \qquad (8)$$

Where k_2 ($g.mg^{-1}.h^{-1}$) is the rate constant of second-order adsorption. The linear plot of t/qt versus t at 20°C, as shown in Figure 13, yielded R^2 values that were greater than 0.978 for all RB concentrations. It also showed a good agreement between the experimental and the calculated qe values (Table 3), indicating the applicability of this model to describe the adsorption process of RB onto EP.

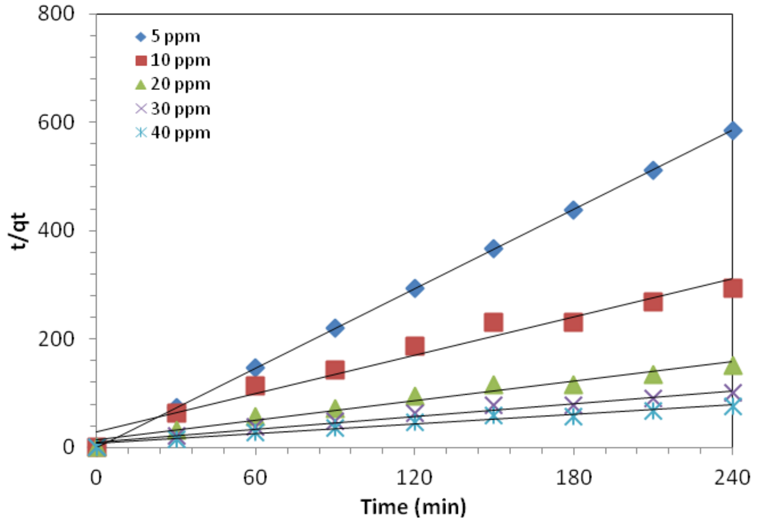

Figure 13: Pseudo-second order kinetic model for RB adsorption onto EP at different initial concentrations

Intra-particle diffusion model based on the theory proposed by Weber and Morris [18] was tested to identify the diffusion mechanism. According to this theory:

$$q_t = K_p t^{1/2} + C \qquad (9)$$

Where C is the intercept and Kp is the intra-particle diffusion rate constant ($mol.min^{-1/2}.g^{-1}$), is obtained from the slope of the straight line of qt versus $t^{1/2}$.

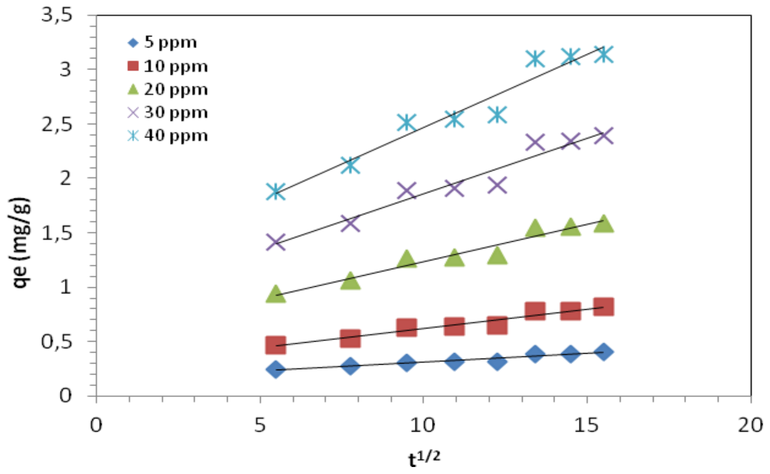

Figure 14: Intra-particle diffusion kinetic model for RB adsorption onto EP at different initial concentrations

Table 3: Pseudo-first-order, Pseudo-second-order and Intra-particle diffusion values

C_0 (mg/L)	qe^{exp} (mg/g)	Pseudo-first-order			Pseudo-second-order			Intra-particle diffusion		
		qe	K_1	R^2	qe	K_2	R^2	C	Ki	R^2
5	0.410	0.626	0.013	0.884	0.410	$-9.91\text{x}10^3$	1.000	0.146	0.017	0.939
10	0.820	0.699	0.031	0.900	0.937	$24\ \text{x}10^3$	0.974	0.268	0.035	0.952
20	1.590	1.223	0.017	0.871	1.839	$13\ \text{x}10^3$	0.977	0.559	0.068	0.945
30	2.390	1.451	1.451	0.873	2.747	$8.76\text{x}10^{-3}$	0.977	0.837	0.102	0.946
40	3.140	1.803	0.022	0.834	3.620	$6.87\text{x}10^{-3}$	0.978	1.136	0.133	0.941

3.7. *Thermodynamic Studies*

Thermodynamic parameters including Gibbs free energy change (ΔG°), enthalpy change (ΔH°), and entropy change (ΔS°) was calculated from the following:

$$\Delta G° = -RT \ln K_d \qquad (10)$$

$$\ln K_d = \frac{\Delta S°}{R} - \frac{\Delta H°}{RT} \qquad (11)$$

Where R is the ideal gas constant (8.314 $J.mol^{-1}.K^{-1}$), T is the absolute temperature (Kelvin), and K_d is the distribution coefficient for adsorption.

Equation (10) is known as the Van't Hoff equation, and it expresses a relationship between equilibrium constant and temperature. Plots of ln K_d versus 1/T (K^{-1}) should be a straight line as shown in Figure 15.

The values of ΔH° and ΔS° were calculated from the slope and intercept of Van't Hoff plot, respectively. The thermodynamic parameters associated with the adsorption of RB onto EP are listed in Table 4. The positive values of ΔG° suggest that adsorption reaction requires energy to carry out [19].

According to the Van't Hoff equation, standard enthalpy and the entropy values in the range of 20–60°C were obtained as 5.051 $kJ.mol^{-1}$ and -0.0056 $kJ.mol^{-1}.K^{-1}$, respectively. The positive value of ΔH° indicates the endothermic nature of the process. The negative ΔS^o value (−0.0056 $KJ.mol^{-1}.K^{-1}$) was caused by the decrease in degree of freedom of the adsorbed species [20], the maximum adsorption capacity increased with an increase in solution temperature from 20 to 60°C. This further confirmed the endothermic nature of the process.

Table 4: Values of thermodynamics parameters for RB adsorption onto EP

Temperature (K)	ΔG ($kJ.mol^{-1}$)	ΔH ($KJ.mol^{-1}$)	ΔS($KJ.mol^{-1}.K^{-1}$)	R^2
293.15	6.7179	5.051	-0.005687	0.8577
303.15	6.7748			
313.15	6.8317			
323.15	6.8885			
333.15	6.9454			

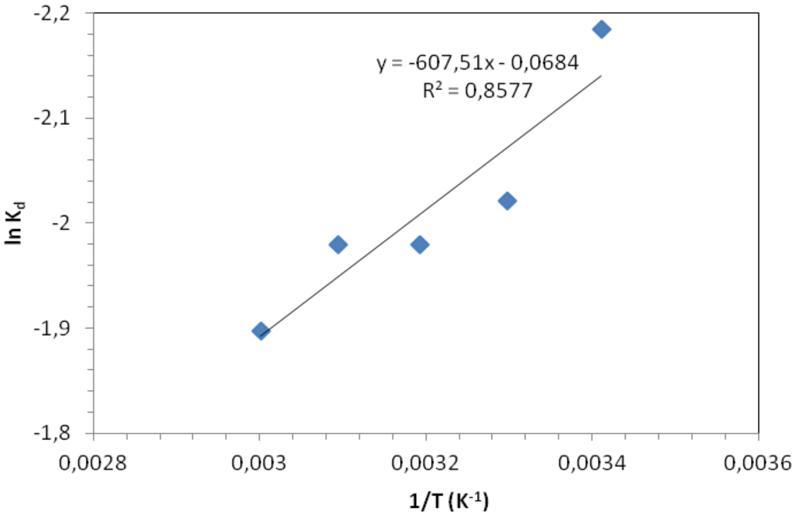

Figure 15: Plot of ln K_d versus 1/T for the enthalpy change of the adsorption process

Conclusion

The present study evaluates that the EP can be used as a promising, effective adsorbent for the removal of RB from wastewater. The adsorption of RB was found to be dependent on the time of contact solution temperature, initial concentration and pH of solution. The maximum removal of RB was found to be 82%.

The equilibrium adsorption data were best represented by the Langmuir isotherm, indication monolayer adsorption on a homogenous surface and values of qmax where increased from 0.39 to 0.49 mg/g. The adsorption kinetic was well described by the pseudo-second-order model. The removal process of RB onto EP is more spontaneous at upper temperatures, tends to be endothermic.

References

1. Banerjee S., Sharma G. C., Dubey S., Sharma Y. C., *J Mater Environ Sci*, 6 (2015), 2045–2052.
2. Abidi N., Duplay J., Elmchaouri A., Jada A., Trabelsi-Ayadi M., *Journal of Colloid Science and Biotechnology*, 3 (2014), 98-110.
3. Gooch J. W., *Polyimide Fiber*. Springer, (2011).
4. Polatli M., Erdinç M., Erdinç E., Okyay E., *Environmental Research*, 86 (2001), 238–43.
5. Doğan M., Alkan M., Çakir Ü., *Journal of Colloid and Interface Science*, 192 (1997), 114–18.
6. Alkan M., Doğan M., *Journal of Colloid and Interface Science*, 243 (2001), 280–91.
7. Sadik C., Albizane A., El Amrani I.E., *J. Mater. Environ. Sci*, 4 (2013), 981–986.
8. Cicero C. A., Bickford D. F., Bennert D. M., Overcamp T. J., *Westinghouse Savannah River Co*, (1994).
9. Doğan M., Alkan M., Onganer Y., *Water, Air, and Soil Pollution*, 120 (2000) 229–248.
10. Mahammedi F., Benguella B., *J. Mater. Environ. Sci*, 7 (2016) 285–292.
11. Ad C., Benalia M., Laidani Y., Elmsellem H., Henini G., Nouacer I., Djedid M., *J. Mater. Environ. Sci*, 7 (2016) 319–330.
12. Langmuir I., *J. Chem. Soc*., 38 (1916) 2221–2295.
13. Abd El-Latif M. M., Elkady M. F., *Desalination*, 255 (2010) 21–43.
14. Freundlich H.M.F., *Physik. Chemie (Leipzig)*, 57A (1906) 385–470.
15. Aharoni C., Ungarish M., *Journal of the Chemical Society, Faraday Transactions 1: Physical Chemistry in Condensed Phases*, 73 (1977) 456–464.
16. Lagergren S., *Kungliga Svenska Vetenskapsakademiens Handlingar*, 24 (1898) 1–39.
17. Ho Y. S., McKay G., *Chemical Engineering Journal*, 70 (1998) 115–24.
18. MORRIS J. C., WEBER W. J., *Advances in Water Pollution Research*, (1964) 231–66.
19. Ali R. M., Hamad H. A., Hussein M. M., Malash G. F., *Ecological Engineering*, 91 (2016) 317–32.
20. Sarı A., Şahinoğlu G., Tüzen M., *Industrial & Engineering Chemistry Research*, 51 (2012) 6877–86.

(2017) ; http://www.jmaterenvironsci.com